Analyzing the Effects of Shear Deformations on the Structural System Identification

Seyyedbehrad Emadi [1]*

[1] DICIV, Department of Civil Engineering, University of Salerno, Fisciano (SA), Italy.

* Correspondence: behradei@gmail.com

Traditional structural system identification techniques often rely on redundant measurement sets due to the linearity of their governing equations, a requirement that becomes problematic when data availability is limited. To mitigate these constraints, more adaptable identification methods have recently been introduced. However, similar to many existing approaches, they are typically based on the Euler–Bernoulli beam theory, which neglects shear deformation effects. While this assumption may be acceptable for slender members, it can lead to significant inaccuracies in elements such as deep beams, where shear contributions strongly influence mechanical properties. This study addresses this limitation by integrating shear deformation into a structural system identification framework. Through a comprehensive parametric analysis, the impact of shear deformation on the structural response across members with varying slenderness ratios is evaluated, offering improved accuracy and reliability for system identification in practical engineering applications.

Keywords: Health monitoring, Structural System Identification, Observability Method, Shear stiffness, beams, bridges.

1. Introduction

System Identification (SI) refers to the process of constructing models for systems whose internal characteristics are not fully known, and it is widely employed across different branches of engineering [1]. The goal is to generate mathematical representations capable of capturing how the system behaves. One of the earliest contributors was Friedrich Gauss, who devised the Gauss–Newton method for refining parameter estimates in orbital trajectory calculations. SI initially emerged in electronic engineering but soon spread into other scientific and technical disciplines [2, 3]. Within SI, Structural System Identification (SSI) is a specific branch that focuses on extracting structural parameters, such as bending and axial stiffness, through mathematical formulations [4].

A broad spectrum of SSI techniques has been proposed in the literature [5, 6]. Classification is typically made by the type of loading used: dynamic tests [7, 8] versus static tests [9]. Another categorization separates parametric approaches [10] from non-parametric approaches [11, 12]. In parametric schemes, models are grounded in structural mechanics, while non-parametric strategies assign parameters numerically, via optimization, without attaching them to physical quantities. The most common formulation used in parametric SSI is the Stiffness Matrix Method (SMM) [13-16]. A detailed overview of such approaches is compiled in [17].

Received: 16 November 2024
Accepted: 09 December 2024
Published: 13 December 2024

Although shear deformation can be critical for certain structural elements, many SSI procedures neglect it. In slender members, shear deflection is typically minor compared to bending, making its omission tolerable. However, for short or deep beams, the influence of shear is substantial, and ignoring it produces what is known as a modeling error. Neglecting this phenomenon leads to inaccurate predictions of system properties. Conventional SSI procedures based on the SMM often rely on elementary beam theory, which disregards shear, thereby underestimating deflections and overestimating natural frequencies [18]. The first attempt to incorporate shear deformation in beam theory is attributed to Timoshenko (1921) [19], whose theory accommodates both bending and shear, though at the expense of mathematical complexity. Because of that complexity, many SSI formulations still rely on the simpler Euler–Bernoulli framework, which ignores shear. Nevertheless, various researchers have attempted to introduce shear considerations into SMM [20, 21].

Recent work extends these ideas. Soto et al. (2017) [22] introduced a shear-inclusive SMM model for fixed-end I-sections. Shear behavior in sandwich plates was explored by Li, J. et al. (2014) [15]. Composite structures combining steel and concrete were studied by Kawano, A. et al. (2019) [23] and Chao, S. et al. (2019) [24]. Tomas et al. (2018) [25] advanced the Observability Method (OM) by incorporating shear deformation into the SMM framework. This was a novel step, as it allowed shear-related equations to be expressed parametrically within OM for the first time. However, the trade-off is that OM requires both vertical displacements and rotational data to retrieve stiffness properties. OM itself is an SSI approach derived from SMM principles, using static deformation measurements to infer structural stiffness. It has proven effective for multiple structural configurations, trusses, beams, frames, and cable-stayed bridges [26-28].

The most detailed attempt to assess shear effects within OM remains the study by Tomas et al. (2018) [25]. Their results revealed that when only vertical deflections from static tests are considered, stiffness properties cannot be correctly identified due to the mathematical form of the governing equations. To achieve accurate results, OM also requires rotational measurements, something rarely captured in practice since infrastructure monitoring usually depends on vertical displacement data, obtained, for example, from surveying, while rotation sensors such as clinometers are used infrequently [29]. Moreover, displacement-based data are typically more robust than rotational measurements, and international standards prioritize vertical deflections as reference. This limitation highlights a critical gap in OM methodology.

Addressing this gap is crucial, as reliable structural assessment methods must balance theoretical completeness with practical feasibility. While OM represents a promising framework, its dependence on rotation data makes it less applicable in real-world monitoring scenarios. Therefore, further research is needed to adapt or extend OM so that meaningful stiffness properties can be derived using only displacement-based information, particularly vertical deflections, which remain the most accessible and standardized measurements. The present study contributes to this effort by examining the role of shear deformation in OM, analyzing its limitations when applied exclusively with vertical deflections, and exploring potential pathways for enhancing the method's applicability in structural health monitoring.

The objective of this study is therefore to clarify why OM cannot reliably determine structural properties when restricted to vertical deflection measurements. To address this, parametric numerical analyses are performed on progressively complex examples. The paper is structured as follows: Section 2 outlines OM with shear considerations; Section 3 applies the approach to a simply supported beam and a cantilever, showing the limitations reported by Tomas et al. (2018) [25]; Section 4 discusses in detail why OM fails under vertical-deflection-only measurements; and Section 5 summarizes the key conclusions

2. Observability Method

From the direct stiffness formulation of a two-dimensional beam element subjected to in-plane loading, the equilibrium at the element nodes can be expressed in matrix form as:

$$[K]\cdot\{\delta\}=\{f\} \tag{1}$$

where the displacement vector {δ} is composed of translational degrees of freedom in the horizontal and vertical directions, along with the nodal rotations. The external load vector {f} includes the corresponding horizontal forces, vertical forces, and applied nodal moments. The global stiffness matrix [K] is assembled from the contributions of the individual beam elements, and its entries reflect the axial stiffness (EA), bending stiffness (EI), and the element length (L), where E is the Young's modulus, I is the second moment of area, and A is the cross-sectional area.

In 1968, Przemieniecki [2] was the first to extend the classical beam stiffness matrix by explicitly accounting for shear flexibility. His formulation introduced a correction factor, denoted as ϕ (the shear parameter), which modifies certain terms of the matrix. The parameter is expressed as:

$$\emptyset = \frac{12EI}{GA_vL^2}\ , \tag{2}$$

Here, Av represents the effective shear area, while G is the shear modulus. The coefficient ν corresponds to Poisson's ratio, as indicated in Eq. (3). A detailed inspection of Przemieniecki's formulation reveals that the shear parameter ϕ appears in the denominator of many stiffness matrix entries, which complicates its use. To address this limitation, Tomas et al. introduced a reformulation by defining a new variable, denoted as the OM shear parameter Q. This parameter provides an alternative representation of shear flexibility and is given by (Eq. 4):

$$G = \frac{E}{2(1+v)}\ , \qquad Q = \frac{\emptyset}{1+\emptyset} \tag{3), (4}$$

Once the original shear parameter ϕ is substituted with the OM shear parameter Q, the modified stiffness formulation can be expressed in terms of Q. The resulting element stiffness matrix for a two-dimensional beam element, incorporating shear flexibility, is written as:

$$[K] = \begin{bmatrix} \frac{EA}{L} & 0 & 0 & -\frac{EA}{L} & 0 & 0 \\ 0 & \frac{12EI}{L^3(1+\emptyset)} & \frac{6EI}{L^2(1+\emptyset)} & 0 & -\frac{12EI}{L^3(1+\emptyset)} & \frac{6EI}{L^2(1+\emptyset)} \\ 0 & \frac{6EI}{L^2(1+\emptyset)} & \frac{EI(4+\emptyset)}{L(1+\emptyset)} & 0 & -\frac{6EI}{L^2(1+\emptyset)} & \frac{EI(2-\emptyset)}{L(1+\emptyset)} \\ -\frac{EA}{L} & 0 & 0 & \frac{EA}{L} & 0 & 0 \\ 0 & -\frac{12EI}{L^3(1+\emptyset)} & -\frac{6EI}{L^2(1+\emptyset)} & 0 & \frac{12EI}{L^3(1+\emptyset)} & -\frac{6EI}{L^2(1+\emptyset)} \\ 0 & \frac{6EI}{L^2(1+\emptyset)} & \frac{EI(2-\emptyset)}{L(1+\emptyset)} & 0 & -\frac{6EI}{L^2(1+\emptyset)} & \frac{EI(4+\emptyset)}{L(1+\emptyset)} \end{bmatrix} \tag{5}$$

When a static load test is carried out, the geometry, boundary conditions, and nodal forces are specified. The unknown structural parameters in the stiffness matrix method (SMM) can then be identified by recording a selected set of displacements. This requires solving an inverse problem. For this purpose, the measured data are grouped into subsets: δ1 and f(1), which are the known parts of the global displacement vector {δ} and force vector {f}, respectively. The remaining components, denoted as δ0 from {δ} and f(0) from {f}, are treated as unknowns. With this partitioning, Eq. (1) can be reformulated as:

$$[K^*]\cdot\{\delta^*\} = \begin{bmatrix} K_{00}^* & K_{01}^* \\ K_{10}^* & K_{11}^* \end{bmatrix}\cdot\begin{Bmatrix}\delta_0^*\\ \delta_1^*\end{Bmatrix} = \begin{Bmatrix} f_0 \\ f_1 \end{Bmatrix} = \{f\}\,, \tag{6}$$

To isolate the unknowns on the left-hand side while retaining the measured quantities on the right-hand side, Eq. (6) can be reorganized as:

$$[B]\cdot\{z\} = \begin{bmatrix} K_{10}^* & 0 \\ K_{00}^* & -I \end{bmatrix}\cdot\begin{Bmatrix}\delta_0^*\\ f_0\end{Bmatrix} = \begin{Bmatrix} f_1 - K_{11}^*\delta_1^* \\ -K_{01}^*\delta_1^* \end{Bmatrix} = \{D\}, \tag{7}$$

In this context, 0 and I represent the zero and identity matrices, respectively. To verify whether the system admits a solution, it is necessary to compute the null space [V] of the coefficient matrix [B]. The condition for compatibility requires that the product [V]T{D} vanishes. When this condition is met, the system can be solved; if not, no solution exists. According to Castillo et al. (2000, 2002) [26, 27], the full set of system solutions (7) follows a general structure that combines a particular solution with contributions from the null space.

$$\{Z\} = \{Z_{\mathrm{p}}\} + [V]\cdot\{\rho\}\,, \tag{8}$$

In the formulation, {Zp} represents a particular solution of system (8), while the term [V]{ρ} encompasses the complete set of solutions to the corresponding homogeneous system. Here, [V] provides a basis for the linear space of solutions, and the elements of {ρ} are arbitrary real numbers that define all possible linear combinations of this basis. A variable can have a unique solution not only when the null space of [V] is empty, but also when the corresponding row of [V] consists entirely of zeros. Therefore, by examining [V] and identifying its null rows, one can determine which variables in {Z} are uniquely defined. Interestingly, if none of the variables in {Z} are fixed by null space, any deflections, forces, or other parameters obtained from the initial OM analysis can be fed back recursively to extract additional parameters. Further details on this iterative procedure are discussed in [5, 19].

The literature indicates that vertical displacement measurements generally provide more reliable data than rotations, and international standards predominantly focus on vertical deformations. This makes it important to critically evaluate the OM, particularly to understand the limitations of measurement sets. Specifically, the OM formulation that includes shear deformation [25] fails to identify any parameters if only vertical displacements are measured. In other words, capturing rotations is essential for the observation of any material property through OM. The following section presents an illustrative example highlighting the inability of OM to determine material parameters using solely vertical deflection data.

3. Analyzing the General Solution

In this section, the null space is examined across a series of increasingly complex examples, focusing on cases where measurement sets contain only vertical displacements. The analysis demonstrates that when shear deformation is considered, OM cannot detect any material properties if only vertical deflections are available.

3.1 Example 1: simply supported beam with vertical deflections

Emadi et al. (2019) [30] evaluated the null space of a simply supported beam 0.6 m in length, discretized into 7 nodes and 6 Timoshenko beam elements (Figure 1). The beam has a uniform cross-section, and all elements share identical properties: Young's modulus, Poisson's ratio, shear area, cross-sectional area, and moment of inertia.

Table 1 summarizes the mechanical and geometric properties adopted for the finite element model of the simply supported beam. The cross-sectional area of the beam is set to 0.1 m², while the effective shear area is slightly smaller, 0.0833 m^2, reflecting the reduction commonly introduced to account for non-uniform shear distribution. The second moment of inertia, which governs bending stiffness, is 0.0083 m^4. Material properties are characterized by a Young's modulus of 27 GPa, representative of typical construction materials such as lightweight concrete or stone, and a Poisson's ratio of 0.25, which indicates moderate lateral contraction under axial loading. These parameters together define the stiffness characteristics of the model and serve as the input for the subsequent structural system identification analysis.

Boundary conditions restrict both horizontal and vertical displacements at node 1 (u1=v1=0, u1 = v1 = 0) and vertical displacement at node 7 (v7=0). The only external load in this numerical test is a concentrated vertical force of 100 kN applied at node 3 (V3=100 kN). Vertical deflections were computed using Midas/Civil, and measurement errors are neglected in this analysis

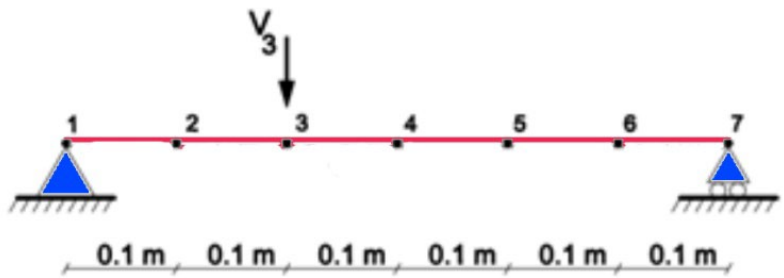

Figure 3. Example 1. FEM for a simply supported beam.

Table 1: Properties of the FEM of the simply supported beam.

Area [m^2]	0.1
Shear Area [m^2]	0.0833
Inertia [m^4]	0.0083
Young's Modulus [GPa]	27
Poisson's Ratio γ	0.25

For the inverse analysis of this structure, the vertical load V3, element lengths, Young's modulus, and Poisson's ratio are treated as known quantities, whereas the moment of inertia I and the shear area Av are considered unknown. Because no horizontal loads are applied in this example, the axial stiffness contributions are not engaged, allowing the corresponding terms in the SMM equations to be omitted. With only III and Av as unknowns in this case, at least two independent deformation measurements would theoretically be required to identify these parameters. However, it is found that no combination of vertical deflections alone is sufficient to accurately recover the unknown.

To demonstrate this limitation, the analysis uses a measurement set consisting of all five vertical deflections available in the beam (from nodes 2 through 6). After applying the variable transformation, the vector of unknowns {Z}, as defined in Eq. (8), includes not only the target parameters I and the OM shear parameter Q, but also additional coupled unknowns, denoted as Iwj and Qw, along with the boundary reactions (H1, V1, V7). The complete solution of this system can then be expressed as:

$$
\begin{bmatrix} I \\ Iw_1 \\ Iw_2 \\ Iw_3 \\ Iw_4 \\ Iw_5 \\ Iw_6 \\ Iw_7 \\ Q \\ Qw_1 \\ Qw_2 \\ Qw_3 \\ Qw_4 \\ Qw_5 \\ Qw_6 \\ Qw_7 \\ H_1 \\ V_1 \\ V_7 \end{bmatrix} = \begin{Bmatrix} 8.0\text{E}-07 \\ 5.0\text{E}-12 \\ 4.0\text{E}-12 \\ 2.0\text{E}-13 \\ 4.0\text{E}-12 \\ 7.0\text{E}-12 \\ 9.0\text{E}-12 \\ 1.0\text{E}-11 \\ 0.0 \\ 0.0 \\ 2.0\text{E}-11 \\ 0.0 \\ 0.0 \\ 0.0 \\ 0.0 \\ 0.0 \\ 0.0 \\ -6.7\text{E}04 \\ -3.3\text{E}04 \end{Bmatrix} + \begin{bmatrix}
1 & \frac{L}{20*(v_5-2*v_6)} & 0 & \frac{-L}{20*(v_5-2*v_6)} \\
0 & \frac{-v_6}{2*(v_5-2*v_6)} & \frac{1}{2} & \frac{v_5-v_6}{2*(v_5-2*v_6)} \\
0 & \frac{-v_6}{2*(v_5-2*v_6)} & \frac{1}{2} & \frac{v_5-v_6}{2*(v_5-2*v_6)} \\
0 & \frac{-v_6}{2*(v_5-2*v_6)} & \frac{1}{2} & \frac{v_5-v_6}{2*(v_5-2*v_6)} \\
0 & \frac{-v_6}{2*(v_5-2*v_6)} & \frac{1}{2} & \frac{v_5-v_6}{2*(v_5-2*v_6)} \\
0 & \frac{-v_6}{2*(v_5-2*v_6)} & \frac{1}{2} & \frac{v_5-v_6}{2*(v_5-2*v_6)} \\
0 & \frac{-v_6}{2*(v_5-2*v_6)} & \frac{1}{2} & \frac{v_5-v_6}{2*(v_5-2*v_6)} \\
0 & \frac{-v_6}{2*(v_5-2*v_6)} & \frac{1}{2} & \frac{v_5-v_6}{2*(v_5-2*v_6)} \\
1 & 0 & 0 & 0 \\
0 & \frac{-2*(v_2-v_3+v_4-v_5+v_6)}{(v_5-2*v_6)} & 0 & \frac{2*v_2-2*v_3+2*v_4-v_5}{(v_5-2*v_6)} \\
0 & \frac{(v_2-2*v_3+2*v_4-2*v_5+v_6)}{(v_5-2*v_6)} & 1 & \frac{-(v_2-2*v_3+2*v_4-2*v_5+v_6)}{(v_5-2*v_6)} \\
0 & \frac{(v_3-2*v_4+2*v_5-2*v_6)}{(v_5-2*v_6)} & 0 & \frac{-(v_3-2*v_4+v_5)}{(v_5-2*v_6)} \\
0 & \frac{(v_4-2*v_5+v_6)}{(v_5-2*v_6)} & 1 & \frac{-(v_4-2*v_5+v_6)}{(v_5-2*v_6)} \\
0 & 1 & 0 & 0 \\
0 & 0 & 1 & 0 \\
0 & 0 & 0 & 1 \\
0 & 0 & 0 & 0 \\
0 & 0 & 0 & 0 \\
0 & 0 & 0 & 0
\end{bmatrix} \cdot \begin{bmatrix} \rho_1 \\ \rho_2 \\ \rho_3 \\ \rho_4 \end{bmatrix} \qquad (9)
$$

As discussed in the previous section (Eq. 8), a variable has a unique solution when the corresponding row in the null space matrix [V] is entirely zero. In this example, the three rows associated with the boundary reactions (H1, H7, and V7) are null, meaning these variables are uniquely determined by the particular solution. In the subsequent recursive step, the parameters that have been identified are fed back into the OM-based SSI procedure. Despite this update to the system of equations, no additional variables can be resolved, and the recursion terminates without yielding further information. Notably, the only parameters successfully observed in this process are the reactions of an isostatic structure, which can be determined directly from equilibrium conditions. This example clearly illustrates that OM is incapable of identifying material or structural parameters when rotations are excluded from the measurement set.

3.2 Example 2: cantilever beam with vertical deflections

Next, a cantilever beam is considered, featuring the same cross-sectional geometry and material characteristics as the simply supported beam previously analyzed.

The cross-section has a total area of 0.1 m², which defines the primary load-bearing surface of the element, while the effective shear area is slightly smaller, at 0.0833 m², to account for the non-uniform distribution of shear stresses across the section. The flexural rigidity of the beam is represented by its second moment of inertia, equal to 0.0083 m⁴, which plays a central role in governing its resistance to bending deformations under external loading. From the material perspective, the elastic response is defined by a Young's modulus of 27 GPa, indicating a relatively stiff behavior typical of lightweight structural materials, whereas the lateral contraction under axial strain is captured by a Poisson's ratio of 0.25, a value consistent with isotropic solids such as aluminum alloys.

By adopting these same geometrical and mechanical parameters for the cantilever case, the comparison with the simply supported configuration remains consistent, enabling a direct evaluation of how boundary conditions, rather than intrinsic material or sectional variations, influence the performance of the observability method when shear effects are taken into account. This structure is discretized into six beam elements and seven nodes, as illustrated in Figure 2.

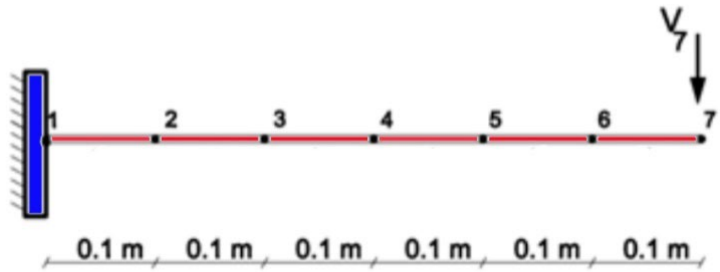

Figure 5. Example 2. FEM for a cantilever beam.

The cantilever beam is constrained at node 1, where all horizontal and vertical displacements, as well as rotational deflections due to bending, are fixed (u1=v1=w1=0). A single concentrated vertical load of 100 kN is applied at the free end, node 7 (V7=100 kN), and the resulting vertical deflections are computed using Midas/Civil.

For the inverse analysis, the applied load V7, element lengths, Young's modulus, and Poisson's ratio are considered known, while the moment of inertia I and the shear area Av are treated as unknowns. Because there are no horizontal forces, axial stiffness effects are inactive, and the corresponding terms in the SMM equations are removed. With only I and Av as unknowns, at least two independent deformation measures would theoretically be required for parameter identification. However, as in Example 1, no combination of vertical deflections alone allows for accurate determination of the unknowns.

This outcome highlights a fundamental limitation of the observability method when applied to systems that include shear deformation. Although the cantilever configuration introduces different boundary conditions compared to the simply supported beam, the lack of rotational information in the measurement set once again prevents the successful identification of both the flexural and shear parameters. The inability to decouple the influence of the moment of inertia from the shear area using only vertical deflections underscores the necessity of incorporating additional types of measurements, such as rotations or mixed deformation data, to achieve a well-posed identification problem. This reinforces the broader conclusion that vertical deflections alone, regardless of structural configuration, are insufficient for capturing the full mechanical behavior of beams when shear effects are non-negligible.

Even though the system of equations can formally be established in this manner, the structure of the solution remains underdetermined when only displacement data are included. In practice, this means that the mathematical framework allows multiple combinations of I and Av to satisfy the same set of vertical deflections, producing ambiguity in the identified parameters. Such indeterminacy not only diminishes the reliability of the observability method but also highlights the importance of integrating richer datasets into the inverse analysis. Incorporating rotations, hybrid load cases, or alternative boundary conditions could provide the additional constraints needed to separate bending and shear effects, thereby yielding more accurate and stable parameter estimates.

To demonstrate this limitation, the analysis uses a measurement set comprising all six vertical deflections from nodes 2 through 7. After the variable transformation, the vector of unknowns $\{Z\}$, as defined in Eq. (8), includes the target parameters I and Q, additional coupled unknowns (Iwj and Qwj), and the boundary reactions (H1, V1, M1. The general solution of this system can then be expressed as:

$$\begin{bmatrix} I \\ Iw_2 \\ Iw_3 \\ Iw_4 \\ Iw_5 \\ Iw_6 \\ Iw_7 \\ Q \\ Qw_2 \\ Qw_3 \\ Qw_4 \\ Qw_5 \\ Qw_6 \\ Qw_7 \\ H_1 \\ V_1 \\ M_1 \end{bmatrix} = \begin{Bmatrix} 8.0\mathrm{E}-02 \\ 2.0\mathrm{E}-7 \\ 3.0\mathrm{E}-7 \\ 5.0\mathrm{E}-8 \\ 5.0\mathrm{E}-7 \\ 6.0\mathrm{E}-7 \\ 6.0\mathrm{E}-7 \\ 0.0 \\ 1.0\mathrm{E}-6 \\ 0.0 \\ 1.0\mathrm{E}-6 \\ 0.0 \\ 1.0\mathrm{E}-6 \\ 0.0 \\ 0.0 \\ -1.0\mathrm{E}05 \\ -6.0\mathrm{E}04 \end{Bmatrix} + \begin{bmatrix} 1 & \dfrac{L}{20 \ast (2 \ast v_2 - 2 \ast v_3 + 2 \ast v_4 - 2 \ast v_5 + 2 \ast v_6 - v_7)} \\ 0 & 0 \\ 0 & 0 \\ 0 & 0 \\ 0 & 0 \\ 0 & 0 \\ 0 & 0 \\ 1 & 0 \\ 0 & \dfrac{-v_2}{(2 \ast v_2 - 2 \ast v_3 + 2 \ast v_4 - 2 \ast v_5 + 2 \ast v_6 - v_7)} \\ 0 & \dfrac{2 \ast v_2 - v_3}{(2 \ast v_2 - 2 \ast v_3 + 2 \ast v_4 - 2 \ast v_5 + 2 \ast v_6 - v_7)} \\ 0 & \dfrac{-(2 \ast v_2 - 2 \ast v_3 + v_4)}{(2 \ast v_2 - 2 \ast v_3 + 2 \ast v_4 - 2 \ast v_5 + 2 \ast v_6 - v_7)} \\ 0 & \dfrac{2 \ast v_2 - 2 \ast v_3 + v_4 - v_5}{(2 \ast v_2 - 2 \ast v_3 + 2 \ast v_4 - 2 \ast v_5 + 2 \ast v_6 - v_7)} \\ 0 & \dfrac{-(2 \ast v_2 - 2 \ast v_3 + v_4 - v_5 + v_6)}{(2 \ast v_2 - 2 \ast v_3 + 2 \ast v_4 - 2 \ast v_5 + 2 \ast v_6 - v_7)} \\ 0 & 1 \\ 0 & 0 \\ 0 & 0 \\ 0 & 0 \end{bmatrix} \cdot \begin{bmatrix} \rho_1 \\ \rho_2 \\ \rho_3 \\ \rho_4 \end{bmatrix} \tag{10}$$

As discussed previously (Eq. 8), a variable is uniquely determined when its corresponding row in the null space matrix [V] consists entirely of zeros. In the case of this cantilever beam, the three rows associated with the boundary reactions (H1, M1, and V1) are null, meaning these reaction forces and moments are uniquely defined by the particular solution. During the subsequent recursive step, these identified parameters are fed back into the OM-based SSI procedure. However, even after updating the system of equations (Eq. 10) with this information, no additional unknowns can be resolved, and the recursion terminates without yielding further insight. Notably, the only parameters that can be observed are the boundary reactions of an isostatic system, which can be directly obtained from equilibrium considerations. This example thus confirms that OM fails to identify material or structural parameters when rotational measurements are excluded from the dataset.

4. Analyzing the Results

As demonstrated in Eqs. (9) and (10), even a large number of measurements fails to allow the OM to identify any material or structural properties. A careful examination of the general solution reveals that the variables in the vector {Z} are highly interdependent, as indicated in Eqs. (11) and (12). Because of this strong coupling, equations that account for rotational effects cannot be effectively solved unless rotational measurements are included in the dataset. This is particularly true for parameters such as I and Q, which are closely linked to rotational degrees of freedom in the system. Mathematically, this coupling is reflected in the fact that the corresponding null space rows are nonzero, meaning these parameters do not have unique solutions.

This outcome highlights a broader implication for the applicability of the observability method: increasing the number of displacement measurements alone does not resolve the identifiability issue. In fact, the redundancy of displacement data only reinforces the same coupling patterns among parameters, leaving the null space unaffected. As a result, the method's inability to isolate shear and flexural properties is not a matter of measurement quantity but of measurement diversity. Without incorporating rotational data or alternative observables, the system remains mathematically ill-conditioned, and parameter identification becomes fundamentally unattainable within the OM framework.

$$Z = \begin{bmatrix} I \\ Iw_1 \\ Iw_2 \\ Iw_3 \\ Iw_4 \\ Iw_5 \\ Iw_6 \\ Iw_7 \\ Q \\ Qw_1 \\ Qw_2 \\ Qw_3 \\ Qw_4 \\ Qw_5 \\ Qw_6 \\ Qw_7 \\ H_1 \\ V_1 \\ V_7 \end{bmatrix}, \qquad Z^* = \begin{bmatrix} I \\ Iw_2 \\ Iw_3 \\ Iw_4 \\ Iw_5 \\ Iw_6 \\ Iw_7 \\ Q \\ Qw_2 \\ Qw_3 \\ Qw_4 \\ Qw_5 \\ Qw_6 \\ Qw_7 \\ H_1 \\ V_1 \\ M_1 \end{bmatrix} \qquad (11), (12)$$

5. Conclusion

Most Structural System Identification (SSI) techniques neglect shear deformation, as it is often small compared to flexural effects. However, in certain structural configurations, shear can have a significant influence. According to the literature, the only comprehensive study that explicitly considers shear effects in static SSI is the Observability Method (OM). Despite this, OM is unable to identify structural parameters when only vertical deflections are measured. To address this limitation, the present study investigates the impact of shear deformations within the OM framework.

Two benchmark cases—a simply supported beam and a cantilever—are analyzed to demonstrate that OM, even when accounting for shear, cannot determine any parameters from vertical deflections alone. To elucidate this limitation, the general solution formulation of the method is presented for both examples. The subsequent analysis of these solutions reveals that the primary weaknesses of OM arise from the complexity of the equation system and its inherent linearity.

Based on these findings, the study concludes that extending the Constrained Observability Method (COM) to include shear deformation provides a potential solution. Since COM employs a numerical optimization-based approach, it can address the issues of variable coupling and linear system constraints, overcoming the limitations observed in the classical OM.

In addition, the study highlights the importance of measurement strategies in SSI. While vertical deflection is the most accessible and widely standardized parameter, it alone cannot capture the coupling between flexural and shear behavior. Incorporating rotation or hybrid measurement techniques could significantly enhance parameter observability, offering more complete structural characterization. This suggests that future monitoring programs should reconsider the exclusive reliance on vertical displacement measurements.

References

[1] Sirca Jr, G.F., & Adeli, H. (2012). System identification in structural engineering. Scientia Iranica, 19(6), 1355-1364.

[2] Przemieniecki, J. S. (1968). *Theory of matrix structural analysis.* Library of Congress Catalog Card Number 67-19151.

[3] Chao, S. H., & Loh, C. H. (2014). Application of singular spectrum analysis to structural monitoring and damage diagnosis of bridges. *Structure and Infrastructure Engineering, 10(6)*, 708–727. https://doi.org/10.1080/15732479.2012.758643

[4] Lozano-Galant, J. A., Emadi, S., Ramos, G., & Turmo, J. (2018). Structural system identification of shear stiffnesses in beams by observability techniques. *40th IABSE Symposium Nantes 2018: Tomorrow's Megastructures* (pp. S24-111–S24-118). International Association for Bridge and Structural Engineers (IABSE).

[5] Lozano-Galant, J. A., Nogal, M., Castillo, E., & Turmo, J. (2013). Application of observability techniques to structural system identification. *Computer-Aided Civil and Infrastructure Engineering, 28*(6), 434–450. https://doi.org/10.1111/mice.12004

[6] Lin, K. C., Hung, H. H., & Sung, Y. C. (2016). Seismic performance of high-strength reinforced concrete buildings evaluated by nonlinear pushover and dynamic analyses. *International Journal of Structural Stability and Dynamics, 16(03)*, 1450107. https://doi.org/10.1142/S0219455414501077

[7] Zarga, D., Tounsi, A., Bousahla, A. A., Bourada, F., & Mahmoud, S. R. (2019). Thermomechanical bending study for functionally graded sandwich plates using a simple quasi-3D shear deformation theory. *Steel and Composite Structures, 32*(3), 389–410. https://doi.org/10.12989/scs.2019.32.3.389

[8] Emadi, S., & Collaborators. (2023). Simplified calculation of shear rotations for first-order shear deformation theory in deep bridge beams. *Applied Sciences (Switzerland, 13*(5), Article 3362. https://doi.org/10.3390/app13053362

[9] López-Colina, C., Serrano, M. A., Lozano, M., Gayarre, F. L., Suárez, J. M., & Wilkinson, T. (2019). Characterization of the main component of equal width welded I-beam-to-RHS-column connections. *Steel and Composite Structures, 32*(3), 337–346. https://doi.org/10.12989/scs.2019.32.3.337

[10] Gracia-Palencia, A. J., Santini-Bell, E., Sipple, J. D., & Sanayei, M. (2015). Structural model updating of an in-service bridge using dynamic data. *Structural Control and Health Monitoring, 22*(10), 1265–1281. https://doi.org/10.1002/stc.1742

[11] Karabelivo, K., Cuéllar, P., Baebler, M., & Rucker, W. (2015). System identification of inverse, multimodal, and nonlinear problem using evolutionary computing: Application to a pile structure supported in nonlinear springs. *Engineering Structures, 101*, 609–620.

[12] Mei, L., Mita, A., & Zhou, J. (2016). An improved substructural damage detection approach of shear structure based on ARMAX model residual. *Structural Control and Health Monitoring, 23*(2), 218–236. https://doi.org/10.1002/stc.1766

[13] Hou, Z., Xia, H., Zhang, Y., Zhang, T., & Y, W. (2015). Dynamic analysis and model test on steel-concrete composite beams under moving loads. *Steel and Composite Structures, 18*(3), 565–582.

[14] Kahya, V., & Turan, M. (2018). Vibration and buckling of laminated beams by a multi-layer finite element model. *Steel and Composite Structures, 28*(4), 415–426. https://doi.org/10.12989/scs.2018.28.4.415

[15] Li, J., Huo, Q., Li, X., Kong, X., & Wu, W. (2014). Dynamic stiffness analysis of steel-concrete composite beams. *Steel and Composite Structures, 16*(6), 577–593. https://doi.org/10.12989/scs.2014.16.6.577

[16] Araki, Y., & Miyagi, Y. (2005). Mixed integer nonlinear least-squares problem for damage detection in truss structures. *Journal of Engineering Mechanics, 131*(7), 659–667. https://doi.org/10.1061/(ASCE)0733-9399(2005)131:7(659)

[17] American Society of Civil Engineers. (2013). *Structural identification of constructed systems*. Reston, VA: American Society of Civil Engineers.

[18] Sayyad, A.S (2011), "Comparison of various refined beam theories for the bending and free vibration analysis of thick beams", Applied and Computational Mechanics, 5, 217–230.

[19] Timoshenko, S. P. (1921). On the correction for shear of the differential equation for transverse vibrations of prismatic bars. *Philosophical Magazine, 41*(6), 742–746. https://doi.org/10.1080/14786442108636264

[20] Arefi, M., Pourjamshidian, M., & Ghorbanpour Arani, A. (2019). Dynamic instability region analysis of sandwich piezoelectric nano-beam with FG-CNTRCs face-sheets based on various high-order shear deformation and nonlocal strain gradient theory. *Steel and Composite Structures, 32*(2), 157–171. https://doi.org/10.12989/scs.2019.32.2.151

[21] Dahake, A., Ghugal, Y., & Kalwane, U. B. (2014). Displacements in thick beams using refined shear deformation theory. *Proceedings of the 3rd International Conference on Recent Trends in Engineering & Technology,* Tamil Nadu, India.

[22] Soto, I.L., Rojas, A.L (2017), "Modeling for fixed-end moments of I-sections with straight haunches under concentrated load", Steel and Composite Structures, 23 (5), 597-610.

[23] Kawano, A., & Zine, A. (2019). Reliability evaluation of continuous beam structures using data concerning the displacement of points in a small region. *Engineering Structures, 180*, 379–387. https://doi.org/10.1016/j.engstruct.2018.11.051

[24] Chao, S., Wu, H., Zhou, T., Guo, T., & Wang, C. (2019). Application of self-centering wall panel with replaceable energy dissipation devices in steel frames. *Steel and Composite Structures, 32*(2), 265–279. https://doi.org/10.12989/scs.2019.32.2.265

[25] Tomas, D., Lozano-Galant, J. A., Ramos, G., & Turmo, J. (2018). Structural system identification of thin web bridges by observability techniques considering shear deformation. *Thin-Walled Structures, 123*, 282–293. https://doi.org/10.1016/j.tws.2017.11.017

[26] Castillo, E., Cobo, A., Jubete, F., Pruneda, R. E., & Castillo, C. (2000). An orthogonally based pivoting transformation of matrices and some applications. *SIAM Journal on Matrix Analysis and Applications, 22*(3), 666–681. https://doi.org/10.1137/S0895479898349720

[27] Castillo, E., Jubete, F., Pruneda, R. E., & Solares, C. (2002). Obtaining simultaneous solutions of linear subsystems of equations and inequalities. *Linear Algebra and its Applications, 364*(1–3), 131–154. https://doi.org/10.1016/S0024-3795(01)00500-6

[28] Lei, J., Nogal, M., Lozano-Galant, J.A., Xu, D., & Turmo, J. (2017). Constrained observability method in static structural system identification. *Struct. Control Health Monit*, 25(1), e2040. https://doi.org/10.1002/stc.2040

[29] Abdo, M. A. (2012). Parametric study of using only static response in structural damage detection. *Engineering Structures, 34*, 124–131. https://doi.org/10.1016/j.engstruct.2011.09.027

[30] Emadi, S., & Collaborators. (2019). Structural system identification including shear deformation of composite bridges from vertical deflections. *Steel and Composite Structures, 32*(6), 731–741. https://doi.org/10.12989/scs.2019.32.6.731